NOAA Technical Memorandum NWS SR-144

NESTED GRID MODEL PERFORMANCE DURING COLD OFFSHORE AND WARM ONSHORE FLOW OVER THE GULF OF MEXICO

Paul R. Janish
EFF/NSSL/CIMMS
Norman, Oklahoma

Steven W. Lyons
Scientific Services Division
Fort Worth, TX

Scientific Services Division
Southern Region
Fort Worth, Texas
October 1992

ED STATES
ARTMENT OF COMMERCE
Barbara Franklin, Secretary

National Oceanic and Atmospheric Administration
John A. Knauss
Under Secretary and Administrator

National Weather Service
Elbert W. Friday
Assistant Administrator

NESTED GRID MODEL PERFORMANCE DURING COLD OFFSHORE AND WARM ONSHORE FLOW OVER THE GULF OF MEXICO

1. Introduction

During the cool season, cold air outbreaks push into the southern United States, across the Gulf coast, and into the Gulf of Mexico. As relatively cool, dry air moves over warmer Gulf water, it is modified significantly. The Gulf of Mexico Experiments (GUFMEX) of 1988 (Lewis et al., 1989) and 1991 were intensive data gathering efforts over the Gulf designed to facilitate the study of air mass modification during times of cold air outbreak as well as the transport of modified polar or tropical air back to the continent during the return flow phase.

The cycle of cold air outbreak and return flow over the Gulf of Mexico has been defined by Crisp and Lewis (1992) as the ***return flow cycle.*** This cycle involves two (2) distinct phases. The first phase of the cycle, known as the offshore flow phase, is defined as the movement of cold/dry air from the continent to the ocean. The second is defined as the movement of warmer/more moist air from the ocean to the continent and is called the onshore (or return) flow phase. The importance of the return flow cycle cannot be overemphasized. Forecasts of temperature, humidity, clouds, and precipitation along the Gulf coast and farther north are directly dependant upon accurate predictions of air mass modification over the Gulf.

Operational forecasters depend heavily on outputs from numerical weather prediction models in preparing their daily suite of products. Since correct simulations of the return flow cycle are critical, an evaluation of Nested Grid Model (NGM) (Phillips, 1979) performance was conducted during the cool season of 1988. Emphasis was placed on determining model strengths and weaknesses during the return flow cycle. Sections 2 and 3 discuss data acquisition, period of study, methods of analysis, and strategies used to evaluate model performance. Section 4 discusses research results, while section 5 lists results of greatest interest to operational forecasters. A conclusion is presented in section 6.

2. Data Acquisition and Study Period

Data used in this study consist of NMC's Regional Analysis and Forecast System's (RAFS) gridded analyses and 24- through 48-h forecasts over a 41 X 38 gridded array defined on a Northern Hemispheric polar stereographic map projection oriented at 60 N, 105 W. Grid spacing is 190.5 km at this location. The gridded data, which were obtained from an NMC archive at NCAR, are not the original NGM C-grid data (91.45 km grid at 60 N), but rather are a subset of the coarser resolution LFM grid, to which the NGM C-grid fields are interpolated for archiving. The period of study encompasses a two month period from 26 January to 27 March 1988, coincident GUFMEX 1988 special observing period.

Parameters available in this data set include temperature and relative humidity at 1000, 950, 900, 850, 800, 750, 700, 500, 300, and 100 mb, as well as geopotential height at 1000, 950, 850,

700, 500, and 300 mb, and meridional wind and zonal wind at 950, 850, 700, 500, and 300 mb. Surface pressure is also included along with mean precipitable water. Data are available every 12-h (0000 UTC and 1200 UTC) during the entire 62 days for each of the 1558 grid points within the domain. Figure 1 shows a 33 X 24 sub-section of the data archive array used in this study which is slightly smaller than the C-grid domain of the NGM. The three-grid structure of the NGM is given in Hoke et al. (1989). Additional details on NGM analyses during this study are given in DiMego (1988) and Hoke et al. (1989).

Observational data used in this study include twice daily (0000 UTC and 1200 UTC) radiosonde data from NOAA/NWS coastal stations during two special extreme cases of 10-14 February and 8-12 March 1988. Special GUFMEX observations (which were not incorporated into the NGM analyses or forecasts), as well as a series of GOES visible satellite images were also used for comparison.

3. Return Flow Cycle

In order to define return flow cycles using NGM grid point data, 16 specific grid points were chosen over the southern United States. These grid points are shown in Fig. 1. Time series of temperature, relative humidity, meridional and zonal wind from NGM analyses, along with daily weather maps, were analyzed over the 16 points for the duration of the study period. These 16 points were then divided into four (4) fences (shown in Fig. 1). Once the four fences were defined, time series, similar to those described above, were computed for each fence by averaging grid points in each. Meridional wind (v) at 950 mb along the Texas coastal fence (Fence 4) was determined to best represent the return flow cycle. Meridional wind (v-wind) was most sensitive to changes in synoptic regimes influencing the Gulf. An example of the meridional wind time series used in defining return flow cycles in this study is given in Fig. 2.

Although a specific return flow event may be characterized initially by an onshore u-wind component, the v-wind component was the better indicator for both offshore and onshore flow phases over fence 4.

3.1.1 Composite Study

From the v-wind depiction of the return flow cycle over fence 4 (Fig. 2), seven (7) events were associated with large meridional wind oscillations and cycles of offshore and onshore flow. Each cycle displayed two (2) phases, as defined by Crisp and Lewis (1992), which can clearly be identified. They include an offshore flow, characterized by a negative v-wind component, and an onshore or "return" flow, characterized by a positive v-wind component. Sub-classification is given in the form of five (5) specific verification periods:

Verification Period 1: Approximate start time of offshore flow. V-wind component is approximately zero (point of change from +v to -v).

Verification Period 2: Approximate time of maximum cold/dry air advection into (T-2) he Gulf. This period coincides with the maximum negative v-wind component.

Verification Period 3: Approximate start time of return flow. V-wind component (T-3) is approximately zero (point of change from -v to +v).

Verification Period 4: Approximate time of maximum return flow of moisture back (T-4) to the continent. This period coincides with the maximum positive v-wind component.

Verification Period 5: Approximate end time of the return flow. The V-wind (T-5) component is approximately zero (point of change from +v to -v).

Again, all verification periods are defined in terms of the 950 mb, meridional wind along the Texas Coast (Fence 4). Hereafter, the above verification periods will be called T-1, T-2, T-3, T-4, and T-5, respectively. In comparison to Crisp and Lewis (1992), T-1, T-2, and T-3 correspond to the offshore flow phase, while T-3, T-4, and T-5 correspond to the onshore flow phase. The time between each period was calculated for each cycle. Composite time averaged between periods for the seven cases analyzed were 27-h (T-1 to T-2), 28-h (T-2 to T-3), 44-h (T-3 to T-4), and 38-h (T-4 to T-5). The entire cycle averaged 137-h (5.7 d). These averages are however, subject to considerable fluctuation due to 12 h data resolution and the limited number of cases analyzed. The purpose of defining verification periods was not to determine specific time averages between "sub-phases" of the return flow cycle, but rather to identify key periods within the return flow cycle for analysis.

The first step in the compositing technique was to apply the definition of each of the five verification periods to each of the seven return flow cycles. These sub-phases are highlighted in Fig. 2 with T-1 through T-5 labeled for the second cycle. The shortest time span for a complete cycle throughout the study period was 96-h (cycle 5), therefore, each of the five verification periods was able to be defined for each of the seven cycles. Meteorological variables including; u- and v-wind components, mixing ratio, relative humidity, temperature, and equivalent potential temperature, were composited relative to each verification period over each of the seven cycles. Respective fields were summed, then divided by the total number of fields used. Hence, if a spatial distribution of mixing ratio relative to T-4 was desired over the entire 33 X 24 gridded array, all of the T-4 periods for all seven cycles would be averaged at each of the 1558 grid points over the NGM data archive domain (see Fig. 2). Results represent mean synoptic patterns for a particular verification period of the return flow cycle.

Because of the 12-h data resolution and the fact that only the v-wind component was used to define the periods, the exact timing of onset for each period may be in slight error. Nonetheless, this technique clearly defines sub-phases of the return flow cycle which can be

analyzed on synoptic scales. In all cases, at least seven (7) synoptic fields (12-h periods) were included in each composite.

3.1.2 Extreme Case

An examination of individual return flow cycles was made in order to see how particular cases compared with the composite. Of these, the most extreme cold air outbreak and return flow event occurred during a 5-day period from 10-14 February 1988. Particular attention was paid to this event to determine whether or not observed features in a single case were similar to those illustrated in the composite over seven events. It also allowed for analysis of the temporal evolution of a cycle. Comparison between this extreme event, other events, and the seven event composite indicated that the composite was a good representation of the overall scenario, while the extreme event had a similar although stronger signature than the composite.

4. Evaluation of NGM Performance

An evaluation of NGM performance during the return flow cycle was conducted with emphasis on moisture, temperature, and wind evolution. Comparisons of NGM 24- and 48-h forecasts with subsequent NGM analyses (used for verification) illustrated model strengths and weaknesses. A comprehensive report on the details of this research is given in Janish (1991) and Janish and Lyons (1992).

Results from both the composite and extreme event suggest that NGM 48-h forecasts of moisture can be in serious error following a cold air outbreak over the Gulf. Advective processes clearly dominate modification processes in NGM forecasts as the cold air outbreak spreads over the Gulf of Mexico. The NGM advects the frontal moisture gradient over the Gulf rather than modifying the air mass over water as is observed.

Dominance of advection over modification in NGM forecasts often results in the moisture gradient being advected out of the NGM C-grid domain. This is not observed in the analysis. As a result, maritime tropical air from the southern Gulf and Caribbean Sea is cut off from having any significant influence during the incipient return flow in model forecasts.

NGM analyses and observations suggest that low-level moisture errors in NGM forecasts result more from shortcomings in model physics than from poor or inadequate model initialization (at least for the cases diagnosed in this study). These shortcomings are also attributable to the NGM's inability to accurately predict observed temperature inversions over the Gulf or inland, particularly during periods of strong onshore (return) flow. This results in an erroneous forecast of precipitable water, depth of the moist layer, and advancement of moisture inland during return flow. It also affects model forecasts of the low-level jet (LLJ).

Part of the error in modifying the boundary layer adequately in the NGM appears to be lack of sufficient evaporation flux over water. Although changes have been made to the NGM in recent years, the model still suppresses the amount of surface evaporation over the ocean to ***half*** its

actual value (in order to suppress spurious precipitation over the Gulf during cold air outbreaks (Junker and Hoke, 1990)). This may inhibit the ability of the NGM to accurately distribute the release of latent heat through the depth of the model's atmosphere. Research by Aubert (1957), Chang et al. (1982) , Pauley and Smith (1988), Reed et al. (1988), and Smith et al. (1984) illustrate the importance for accurate heat release in the vicinity of developing cyclones in numerical weather prediction models. Preliminary analyses of NGM performance during the 1992 cool season indicate similar biases to those during 1988.

Even though errors documented thus far appear to be related to deficiencies in NGM physics, operational forecasters should always compare model initial fields with upper air and satellite charts prior to reviewing model output. After all, if, for a particular case, the model has problems with initialization, those problems will likely be compounded in forecasts.

When preparing forecasts during periods of return flow, forecasters should examine low-level gridded wind fields and boundary layer specific (or relative) humidities to analyze moisture field evolution during the cycle. Since the NGM is deficient in modifying an air mass as it moves over Gulf waters, particular attention should be placed on cases where return flow is primarily comprised of modified maritime (mP) or modified continental polar (cP) air. In such cases air that returns will be significantly more moist than model forecasts of moisture return. Also, when the NGM is initialized with a north wind and moisture gradient over the coastal zone (ie, during or slightly after frontal passage into Gulf), advective processes will dominate, resulting in forecasts which are excessively dry over the Gulf. In such cases, the moisture gradient is advected too far south over the Gulf. As a result, maritime tropical (mT) air which typically resides over the southern Gulf and northwest Caribbean Sea is displaced farther south as well. This inhibits the amount of tropical air which can return during the initial development of onshore flow along the Gulf coast and northward.

Impacts of moisture deficiency on model quantitative precipitation forecasts (QPF's) during return flow episodes have yet to be fully determined, however, potential underestimations of QPF (especially over south Texas, where deficiencies are typically greatest) correspond well with findings of Junker and Hoke (1989) who note that the NGM underpredicts heavy precipitation over the southern U.S. during times of strong southerly flow.

Diagnostics of temperature evolution during cold air outbreaks revealed several features. The NGM is slow in its initial development of the offshore flow in the lee of the Rockies and over the southern Plains. The strength of the cold surge is typically too weak, and southward penetration of the cold front too slow, during T-1 and T-2. These biases are less apparent during T-3, although they still persist. During periods of strong onshore flow, ageostrophic temperature advection plays a major role in northward temperature transport. At times, ageostrophic temperature advection exceeds geostrophic temperature advection, especially in the vicinity of the LLJ over south Texas during T-4. The NGM accounts for significant ageostrophic temperature advection over Texas, however it is still weaker than verifying analyses indicate.

The NGM does a good job in forecasting wind behind the front during T-2, however it has some difficulty in developing the return flow, especially as it relates to LLJ formation during T-3 and T-4. Although several types of LLJ's have been studied in the literature, Djuric and Damaini (1980) and Djuric and Ladwig (1983) have evaluated LLJ development in association with the return flow cycle. This study examined LLJ formation using the NGM during such periods and focuses primarily on the onshore flow phase.

Prior to the onset of strong onshore flow across the Gulf Coast (T-4), a precursor to the LLJ is observed over the south central Plains at T-3. NGM analyses indicate that the LLJ begins to develop at T-3 over eastern New Mexico and the Texas Panhandle. This jet forms in response to three features. ***First***, the polar anticyclone near 850 mb over south Texas moves offshore into the western Gulf which develops a synoptic flow from the southwest over the Texas Panhandle. ***Second***, a lee mountain trough is present which enhances southwesterly geostrophic wind over the same area. ***Finally, and most importantly***, the jet accelerates in association with a strong isallobaric, ageostrophic wind from the south directed toward rapid pressure falls in the lee of the Rockies. These pressure falls are observed at the surface, but are most pronounced at 850 mb. The lee trough is always present in cases of LLJ formation; however, its presence alone does not initiate LLJ development. Only after synoptic scale winds become southwesterly, and deepening of the lee trough initiates a strong isallobaric, ageostrophic wind from the south, will a jet begin to develop. These processes are observed near the base of the inversion during T-3. NGM forecasts of LLJ development are hindered by difficulties in forecasting these three features. One primary reason for poor LLJ forecasts appears to be the NGM's bias in developing cyclones over the central Plains during such events. Pressure falls and lee cyclogenesis are significantly farther north in NGM forecasts than are observed. Misplaced lee cyclogenesis in the NGM is corroborated by Grumm and Siebers (1989), and Mullen and Smith (1990).

As the LLJ develops, it expands in spatial coverage and forms/develops south and east. It reaches the western Gulf some 18-36 h after its initial formation over eastern New Mexico. Upon reaching the western Gulf, the LLJ is characterized by an upward slope. Namely, maximum winds occur at 950 mb over the western Gulf and at 850 mb over the south central Plains (coincident with the slope of the inversion) during T-4. While this jet does display somewhat of a diurnal maximum (typically strongest at night when the boundary layer inversion is typically strongest) it usually persists throughout the day unlike the summertime LLJ as discussed by Blackadar (1957), Bonner (1968), and Wexler (1961). Formation processes of these two jets show significant dissimilarities and should be thought of separately when making forecasts.

Finally, NGM analyses were compared with satellite data and rawinsonde observations (RAOB's) at collocated points to determine analysis quality (Engel, 1991). Results indicate that analyses depict temperature and moisture profiles (including inversion layers) which are very similar to those observed at specific points. These comparisons were made prior to and during maximum onshore flow. Although somewhat smoothed, profiles in analyses are in good agreement with RAOB and satellite derived data. Thus, for these cases, NGM analyses served as realistic verification arrays for NGM forecasts.

Final upgrades to the NGM physics package were implemented 7 November 1990. These changes included improvements to the soil moisture profile along coastal zones, enhanced orography, inclusion of stability dependent surface fluxes over water, expansion of the C-grid southward to Panama, and a fourth order difference scheme to improve the model spatial resolution (Petersen et al., 1991). Model performance following these changes needs to be examined to determine their influence on the NGM's ability to forecast the return flow cycle. Also, new regional data assimilation which incorporates a new first guess should be examined. Nonetheless, preliminary studies of moisture field evolution during the spring of 1992 indicate that the impact of model changes was minimal and that deficiencies found in 1988 persist today. The NGM is now frozen (no model changes will occur) in order to develop a stable set of model output statistics (MOS). Thus, the strengths and weaknesses illustrated here will likely persist in future model runs.

5. Operational implications

While the NGM provides detailed guidance to operational forecasters during the return flow cycle (both offshore and onshore phases), its use can be enhanced by noting model biases, model deficiencies, pattern evolution, and applying conceptual models to forecasts. The features illustrated above will impact a wide number of forecast decisions related to aviation interests, coastal and marine forecasts, moisture return, temperature forecasts, QPFs, and severe weather potential. These topics need to be addressed individually; however, generalizations can be made from the results of this study. In summary, an evaluation of the NGM during the return flow cycle has shown several strengths and weaknesses. These features are outlined below.

MOISTURE FIELD EVOLUTION:

(1) The NGM tends to advect frontal moisture gradients and invading air masses over the Gulf without modifying them adequately. This impacts marine forecasts of the boundary layer which is usually more moist then predicted by the model. Figure 3 shows the 950 mb analysis and 48 h moisture forecasts from T-3 and T-4. Notice how the packing and orientation of the isohumes differ between Fig. 3a and b with less modification indicated in the forecast. Deficiency in the moisture return is illustrated in Figs. 3c and d. These features are smoothed for the composite of cases. On an individual basis, the features illustrated here are significantly exaggerated. Figure 4 shows the evolution of return flow cycle for an extreme case which illustrates the deficiencies in moisture modification more graphically.

(2) As a result of inadequate air mass modification during offshore flow, return flows involving modified mP air masses will be too dry. This impacts QPF's, precipitable water forecasts, and coastal cloud/fog forecasts. Return flow air masses are significantly drier in NGM forecasts than are typically observed. Figure 5 shows a mixing ratio difference field between NGM 48 h forecasts and NGM analysis for T-3 and T-4. Moisture deficiencies prior to and during maximum return flow are clearly evident.

(3) Moisture content in return flows which involve mT air masses, especially those which move subtly northward along the Sierra Madre Oriental Mountains, are usually underestimated in NGM forecasts. Although Fig. 5 represents a composite, maximum deficiencies are located along the Sierra Madre Oriental Mountains of northeast Mexico.

(4) Long return flow cycles which evolve over several days (versus those which turn from offshore to onshore rapidly) will likely be better forecast. If the model is initialized with near calm or light southerly winds versus northerly winds (during the offshore flow phase), forecasts of moisture return are likely to be better.

(5) Moisture deficiencies during onshore flow are greatest over south Texas and the western Gulf of Mexico, however, deficiencies extend into the central Plains (Fig. 5b).

TEMPERATURE FIELD EVOLUTION:

(1) During the onset of offshore flow, the NGM moves fronts and air masses southward too slowly. This bias is also noted over the central Plains. Forecasts of southward frontal advance can lag 12 h or more behind observations for a 48-h forecast. This lag appears to be largest for air masses which are shallow and cold. Figure 6 shows the forecast frontal lag for T-2. Note that amplitude and strength of the cold surge are less in the forecast as compared to the analysis.

(2) The NGM has difficulty in developing inversion layers near the top of the boundary layer. This adversely affects forecasts of moist layer depth, LLJ, and thermodynamic profile of the return flow. This deficiency is most pronounced during periods of strong onshore flow.

WIND FIELD EVOLUTION:

(1) The LLJ first develops in the Texas Panhandle some 18-36 hours prior to reaching the western Gulf of Mexico. Once the jet forms near the Texas Panhandle, it develops south and east toward the Gulf. It is not until the jet reaches the Gulf that deep moisture advection into the southern Plains is established. Low-level moisture usually returns first along the LLJ axis over central Texas into west-central Oklahoma near 850 mb before the onset of deeper moisture return is observed region wide. Examination of NGM gridded moisture fields (particularly specific humidity) near LLJ level (typically near 850 mb over the central Plains) should aid forecasters in determining whether or not the model has a good handle on moisture return.

(2) Geopotential height and wind are shown in Fig. 7 for T-3. LLJ formation processes are clearly evident in Fig. 7a. Observations indicate that southerly flow has already developed over the Texas Panhandle at this time while model forecasts of southerlies have not developed. The ageostrophic (isallobaric) acceleration of wind over this region is significantly stronger in the analysis (Fig. 7c) than in the forecast (Fig. 7d).

(3) The LLJ displays a slope increasing in height from the Gulf of Mexico northward during it's mature phase. Figure 8, which displays geopotential height and wind for T-4, illustrates this slope. Winds are maximum near 850 mb over the central Plains (Fig. 8a) but are maximum near 950 mb over the western Gulf of Mexico (Fig. 8c). NGM forecasts do not resolve this sloping character of the LLJ (Figs. 8b,d).

(4) Although NGM wind forecasts are generally weaker and more westerly than observed (especially over Oklahoma and Texas), the timing of return flow (winds only) is generally good (Fig. 8). Forecasters should note that while timing may be good, moisture forecasts are usually significantly deficient which will impact many other parameters.

(5) During periods of strong southerly flow, NGM forecasts display a significant northward displacement of surface cyclones as compared to verifying analyses. As a result, initial and subsequent LLJ formation, including both strength and magnitude, over the southern U.S., will be in error. This likely impacts the type and distribution of significant weather associated with developing cyclones during their development and movement across the central Plains. Pattern recognition and incorporation of conceptual models is necessary to enhance forecasts during these events. Figure 8 indicates that analyzed near surface cyclones are located considerably further south than NGM forecast cyclone positions.

6. Conclusions

Integration of these findings into forecast procedures should improve operational decisions. Figure 9 shows schematic diagrams of model strengths and weaknesses associated with the three most important verification periods of the return flow cycle, namely T-2, T-3, and T-4.

During T-1 and T-2, the NGM lags in the southward frontal progression and associated air mass across the central and southern Plains. The amplitude and strength of the cold surge are damped in NGM forecasts, particularly along the front range of the Rockies and over the southern Plains during T-2 (Fig. 9a). Maximum offshore flow along the Texas coast is occurring at this time in association with strong cold air advection. The 950 mb front extends from near New Orleans southward into the central Gulf, significantly east of the NGM 48 h forecast position.

By T-3 (Fig. 9b) the NGM 48 h forecast warm bias shifts east with maximum differences located over the upper Midwest. The 950 mb anticyclone is analyzed over south Texas while the forecast is significantly southwest of this position. A moisture deficiency is observed over the entire Gulf, maximum over the western Gulf. A lee trough develops at 850 mb and, in concert with height falls over the central Rockies, an ageostrophic (isallobaric) wind accelerates from the south over the Texas Panhandle and slightly west. This initiates LLJ development. The jet reaches the Gulf Coast 18-36 h later (Fig. 9c) and displays a slope upward with height as it advances from the western Gulf northward. This feature is absent in NGM forecasts which

show maximum low level winds near 850 mb at all locations. Winds veered along the LLJ axis in NGM forecasts much more than in verifying analyses. The 850 mb trough axis is fairly well predicted, however it is slightly stronger in NGM forecasts resulting in enhanced pressure gradients across the upper Midwest. The surface cyclone is forecast much farther north than analyses indicate. Moisture deficiencies extend northward from the Gulf at T-4 across Texas, Oklahoma, southwest Kansas, and southeast Colorado with maximum values over northeast Mexico and south Texas.

ACKNOWLEDGEMENTS

The author would like to thank Dr. James Scoggins and The Cooperative Institute for Applied Meteorological Studies at Texas A&M University for the support and technical guidance in preparing this report. Also, discussions and reviews by Dr. Dusan Djuric (TAMU), Dr. John Lewis and Mr. Charlie Crisp (NSSL), Mr. Steven Weiss (NSSFC), Dr. Robert Merrill (CIMSS), Mr. Michael Branick (EFF/NWS), Mr. Dan Smith (SSD/SRH), Dr. Kenneth Mitchell (NMC), and others helped frame this research into a proper scientific and operational perspective. Thanks are also extended to Ms. Joan Kimpel (NSSL) for her drafting of the schematic figures.

This effort was funded by the Cooperative Institute for Mesoscale Meteorological Studies (CIMMS) at the University of Oklahoma, the National Severe Storms Laboratory, Texas A&M University, and the National Weather Service - Southern Region, NOAA award No. NA90AA-H-ME797.

REFERENCES

Aubert, E. F., 1957: On the release of latent heat as a factor in large scale atmospheric motions. *J. Meteor.*, **14**, 527-542.

Blackadar, A. K., 1957: Boundary layer wind maxima and their significance for the growth of nocturnal inversions. *Bull. Amer. Meteor. Soc.*, **38**, 283-290.

Bonner, W. D., 1968: Climatology of the low-level jet. *Mon. Wea. Rev.*, **96**, 833-850.

Chang, C. B., D. J. Perkey, and C. W. Kreitzberg, 1982: A numerical case study of the effects of latent heating on a developing wave cyclone. *J. Atmos. Sci.*, **39**, 1555-1570.

Crisp, C. A. and J. M. Lewis, 1992: Return flow in the Gulf of Mexico, Part I: A classificatory approach with a global historical perspective. *J. Appl. Meteor.* (accepted for publication, to appear August 1992).

DiMego, G. J., 1988: The National Meteorological Center's regional analysis system. *Mon. Wea. Rev.*, **116**, 977-1000.

Djuric, D., and M. S. Damiani, Jr., 1980: On the formation of the low-level jet over Texas. *Mon. Wea. Rev.*, **108**, 1854-1865.

Djuric, D., and D. S. Ladwig, 1983: Southerly low-level jet in the winter cyclones of the Southwestern Great Plains. *Mon. Wea. Rev.*, **111**, 2275-2281.

Engel, G. T., 1991: Low-level wind maxima over the western Gulf of Mexico and their role in water vapor advection. M.S. Thesis, Department of Meteorology, Texas A&M University, *CIAMS Report No. 9109-2*, 122 pp.

Grumm, R. H. and A. L. Siebers, 1989: Systematic surface cyclone errors in NMC's nested grid model November 1988 - January 1989. *Wea. Forecasting*, **4**, 246-252.

Hoke, J. E., N. A. Phillips, G. J. DiMego, J. J. Tuccillo, and J. G. Sela, 1989: The regional analysis and forecast system of the Nested Grid Model. *Wea. Forecasting*, **4**, 323-334.

Janish, P. R., 1991: Performance of the Nested Grid Model during cold air outbreaks and periods of return flow. M.S. Thesis, Department of Meteorology, Texas A&M University, *CIAMS Report No. 9109-1*, 157 pp.

Janish, P. R. and S. W. Lyons, 1992: NGM performance during cold air outbreaks and periods of return flow over the Gulf of Mexico with emphasis on moisture field evolution. *J. Appl. Meteor,* Vol. 31, No. 8, 995-1017.

Lewis, J. M., C. M. Hayden, R. T. Merrill, and J. M. Schneider, 1989: GUFMEX: A study of return flow in the Gulf of Mexico. *Bull. Amer. Meteor. Soc.*, **70**, 24-29.

Mullen, S. L., and B. B. Smith, 1990: An analysis of sea level cyclone errors in NMC's Nested Grid Model (NGM) during the 1987-1988 winter season. *Wea. Forecasting*, **5**, 433-447.

Pauley, P. M., and P. J. Smith, 1988: Direct and indirect effects of latent heat release on a synoptic scale wave system. *Mon. Wea. Rev.*, **116**, 1209-1235.

Petersen, R. A., G. J. DiMego, J. E. Hoke, K. E. Mitchell, J. P. Gerrity, R. L. Wobus, H-M. H. Juang, and M. J. Pecnick, 1991: Changes to NMC's regional analysis and forecast system. *Wea. Forecasting,* **6**, 133-141.

Phillips, N. A., 1979: The Nested Grid Model. *NOAA Tech. Report NWS 22*, U. S. Department of Commerce, Washington, D. C., 80 pp.

Reed, R. J., A. J. Simmons, M. D. Albright, and Per Unden, 1988: The role of latent heat release in explosive cyclogenesis: Three examples based on ECMWF operational forecasts. *Wea. Forecasting*, **3**, 217-229.

Smith, P. J., P. M. Dare, and S. J. Lin, 1984: The impact of latent heat release on synoptic-scale vertical motions and the development of an extratropical cyclone system. *Mon. Wea. Rev.*, **112**, 2421-2430.

Wexler, H., 1961: A boundary layer interpretation of the low-level jet. *Tellus*, **13**, 368-378

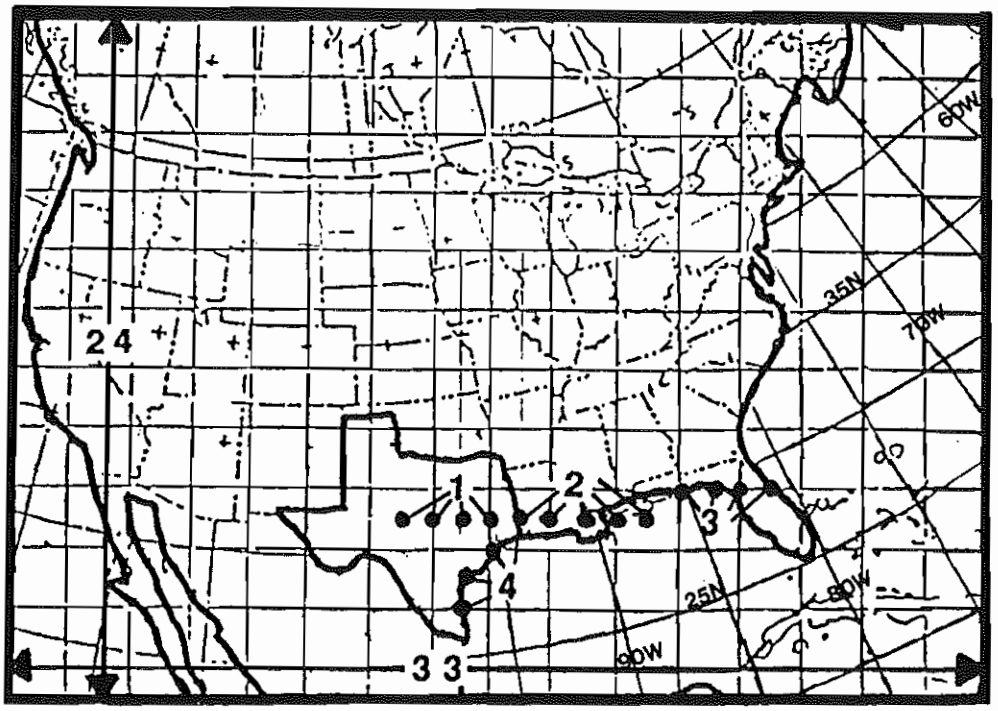

Fig. 1. A 33 X 24 section of the NGM data archive grid over North America. The numbered regions indicate boundaries or "fences" along the coast used to identify the return flow cycle.

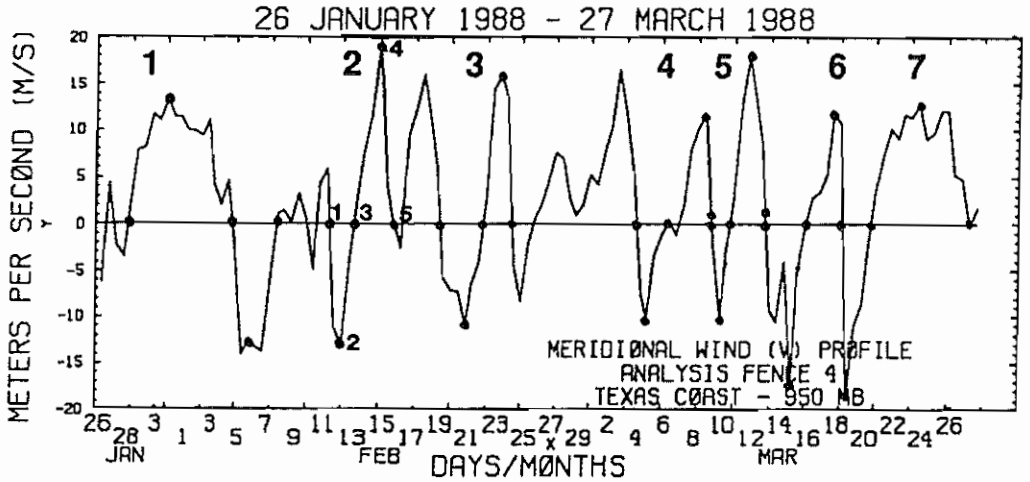

Fig. 2. A time series of the meridional wind component (v) at 950 mb along the Texas Coastal Fence (Fence 4). Seven cycles are indicated. The approximate verification periods for cycle 2 are given.

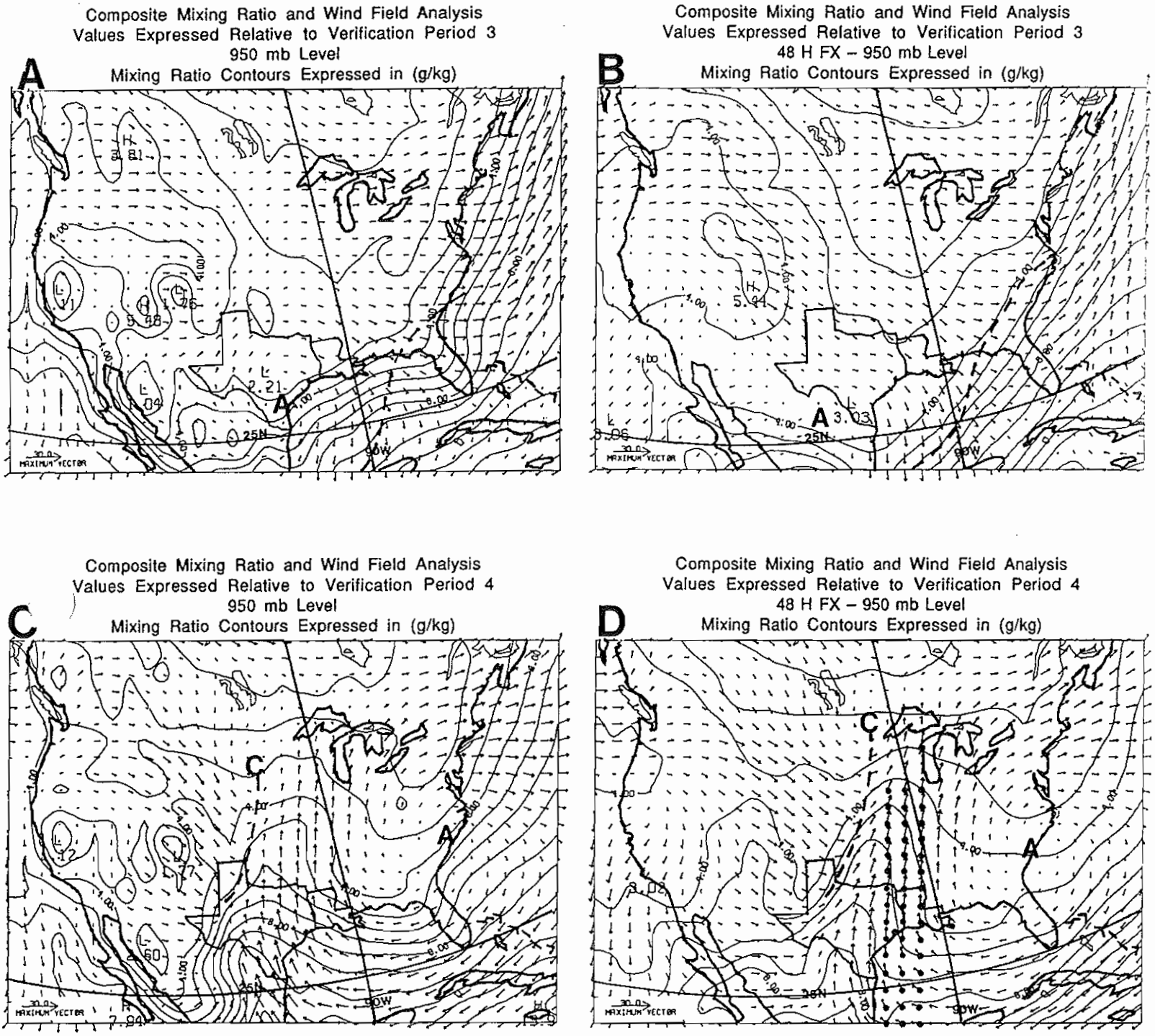

Fig. 3. Mixing ratio and wind at 950 mb for NGM analyses (3(a,c)) and NGM 48 h forecasts (3(b,d)). Charts correspond to verification periods 3 (top) and 4 (bottom) of the composite study. The dashed lines in Figs. 3a and 3b represent the expected position of the 4 g kg^{-1} isohume based on horizontal advection along trajectories from the previous verification period. Positions of cyclones and anticyclones are marked by a "C" and an "A" respectively with frontal positions marked appropriately. Mixing ratio contour interval is 1 g kg^{-1}. The maximum wind vector is given in m s^{-1} in the lower left. The forty-five (45) grid values highlighted in Fig. 3d indicate the axis of vertical cross sections which were analyzed during the study.

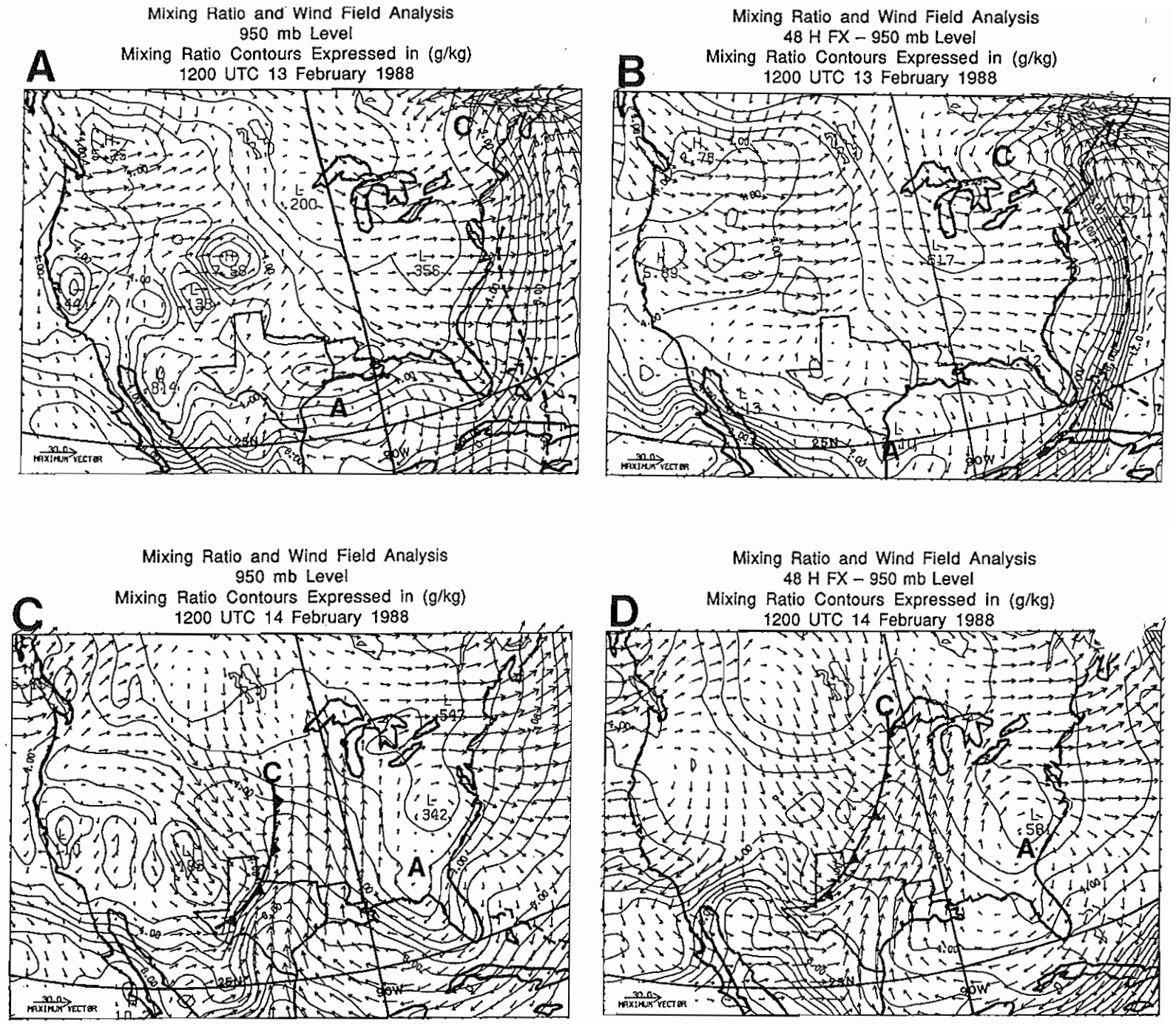

Fig. 4. As Fig. 3 except for 1200 UTC 13 February 1988 (4a (top), similar to T-3) and 1200 UTC 14 February 1988 (4c (bottom), similar to T-4. NGM 48-h forecasts valid at corresponding times are given in Figs. 4(b,d) respectively.

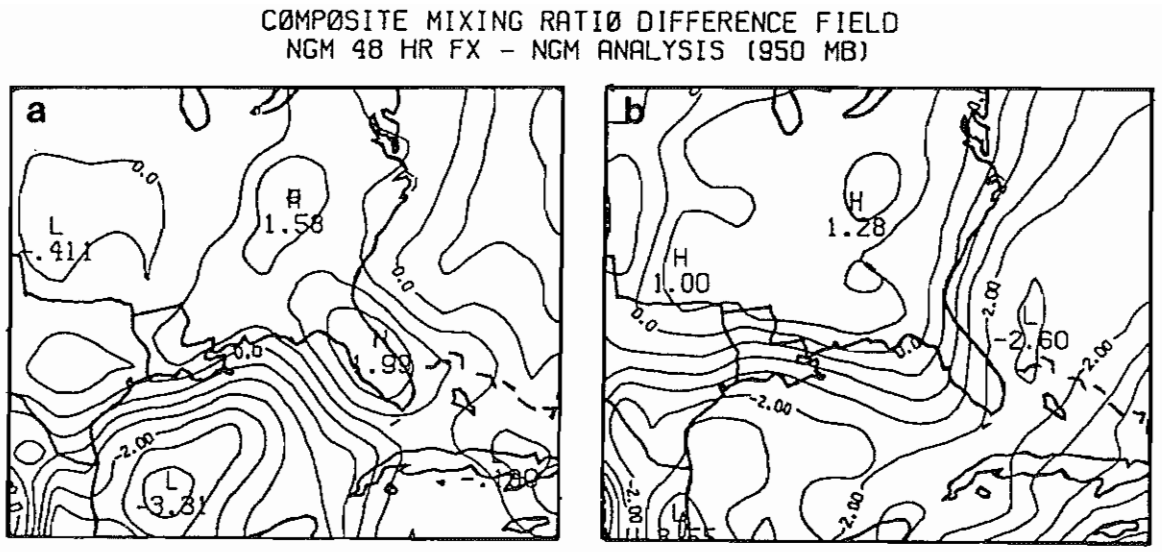

Fig. 5. Mixing ratio difference fields between the NGM 48 h forecast and NGM analysis at 950 mb. Values are expressed as forecast minus analysis, with a contour interval of 0.5 g kg^{-1}. Verification periods 3 and 4 are represented by Figs. 5a and 5b, respectively.

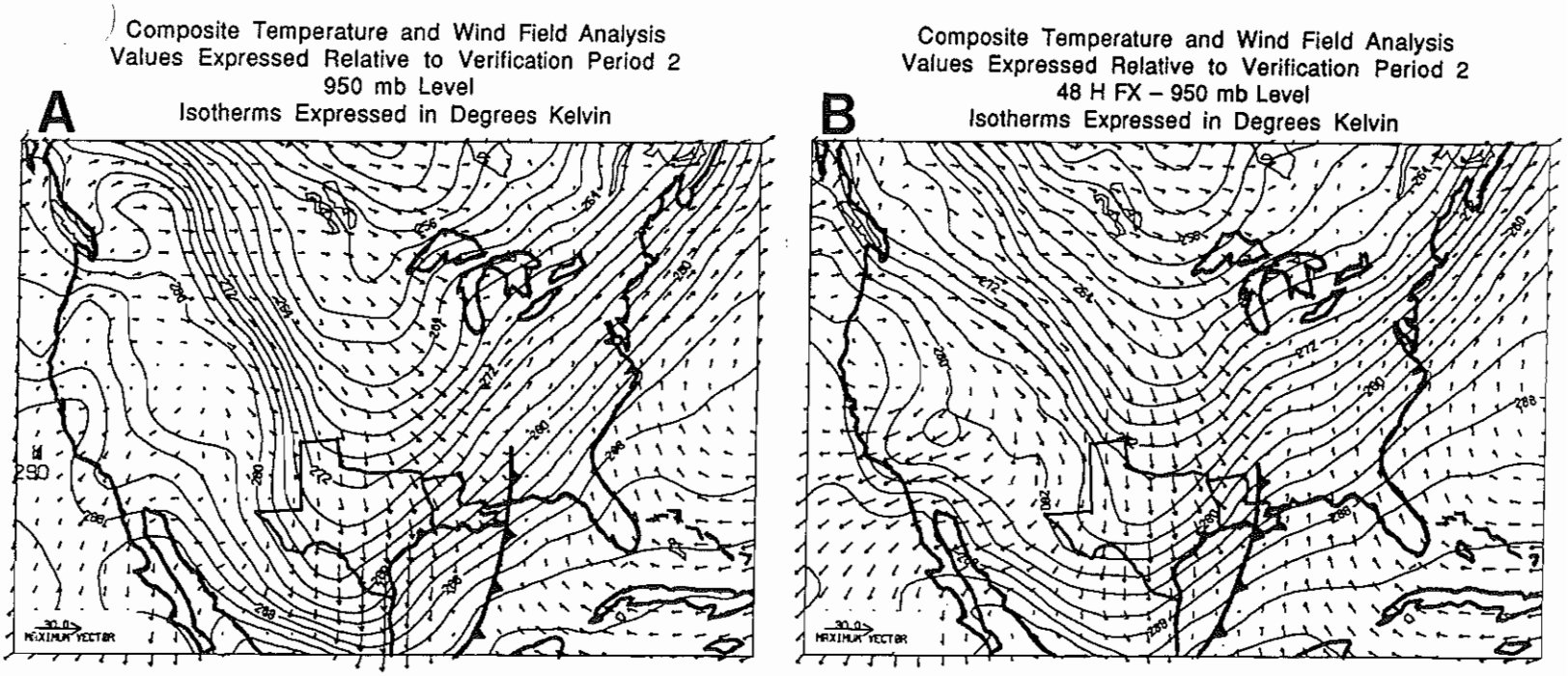

Fig. 6. Temperature and wind at 950 mb for the analysis (Fig. 6a) and NGM 48 h forecast (Fig. 6b) for verification period 2. Positions of cyclones and anticyclones are represented by a "C" and an "A" respectively, with frontal positions marked appropriately. The contour interval is 2 K.

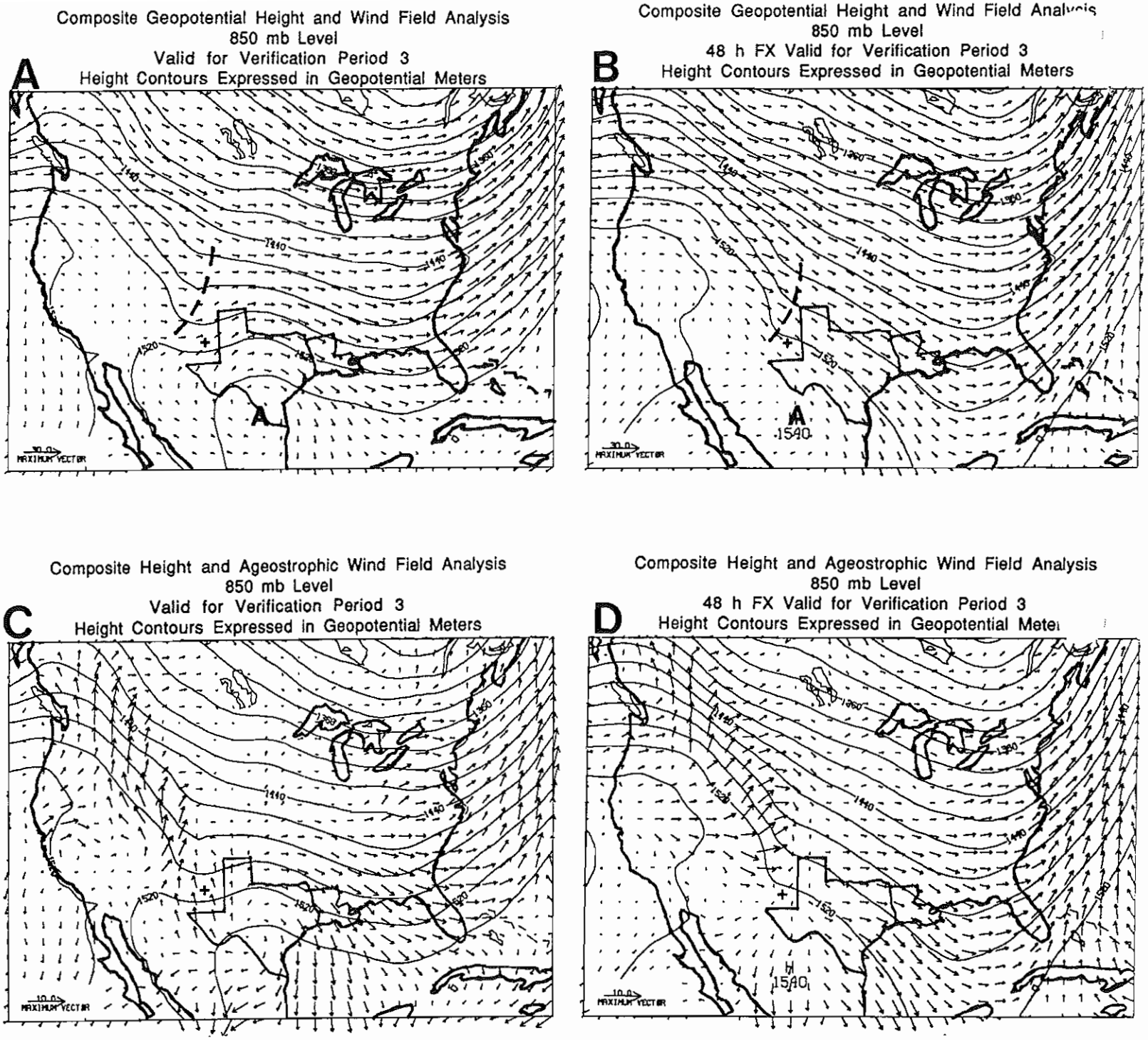

Fig. 7. 850 mb geopotential height and wind composites for NGM analyses and 48 h forecasts. Height field and total wind for T-3 is given in Figs. 7a and 7b. Heights and ageostrophic winds for T-3 are given in Figs. 7c and 7d. Cyclone and anticyclone positions are marked with a "C" and an "A" respectively. The 850 mb trough axis is indicated by the dashed line with the contour interval being 20 gpm, and the maximum wind vector given in m s^{-1} at the lower left. Asterisks are given for points of reference.

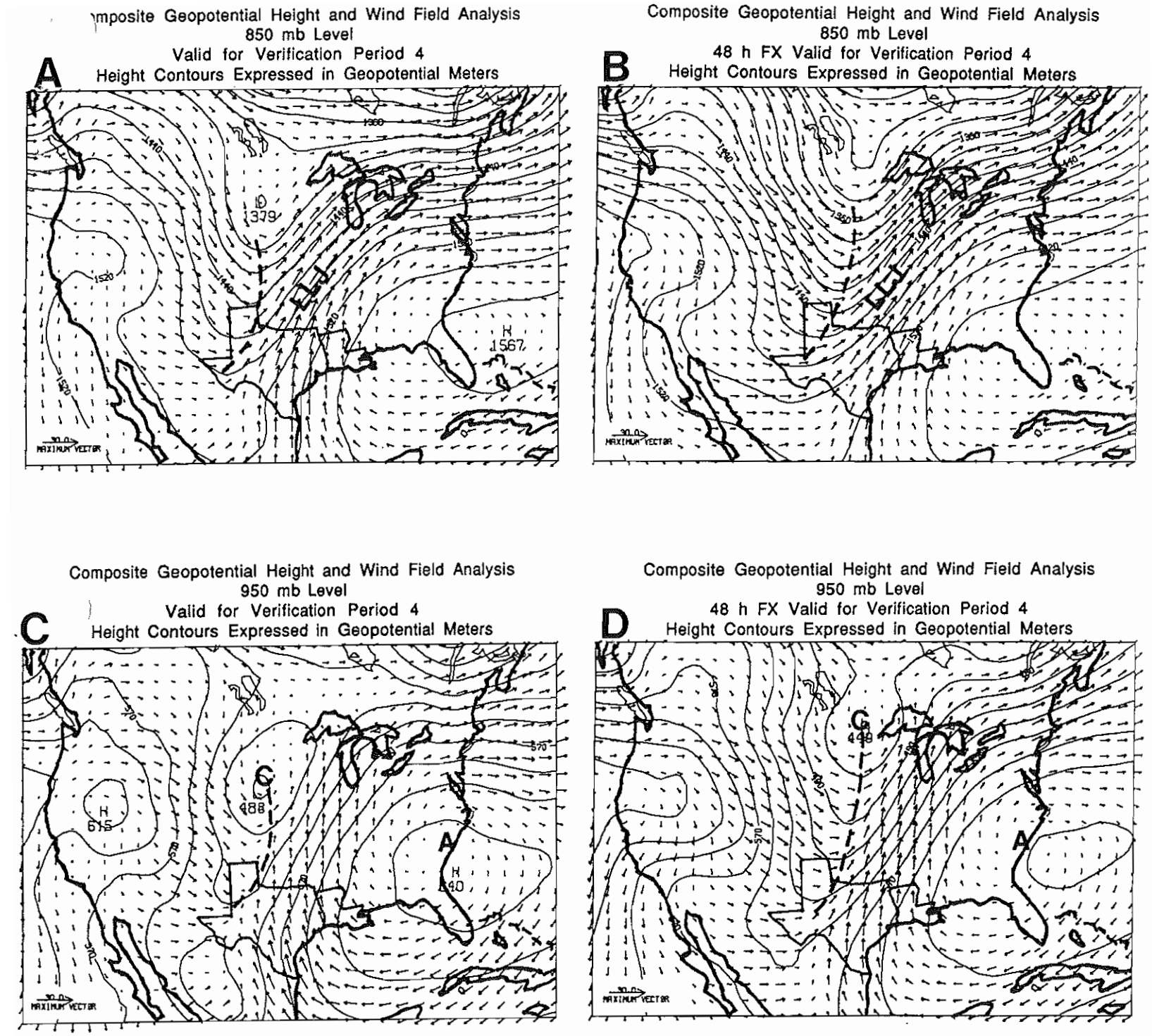

Fig. 8. Geopotential height and wind composites for NGM analyses and 48 h forecasts at T-4. Figs. 8a and 8b give the analysis and forecast at 850 mb while Figs. 8c and 8d give the analysis and forecast at 950 mb. Cyclone and anticyclone positions are marked with a "C" and an "A" respectively. Trough axes are indicated by a dashed line. The contour interval is 20 gpm with the maximum wind vector given in m s^{-1} at lower left.

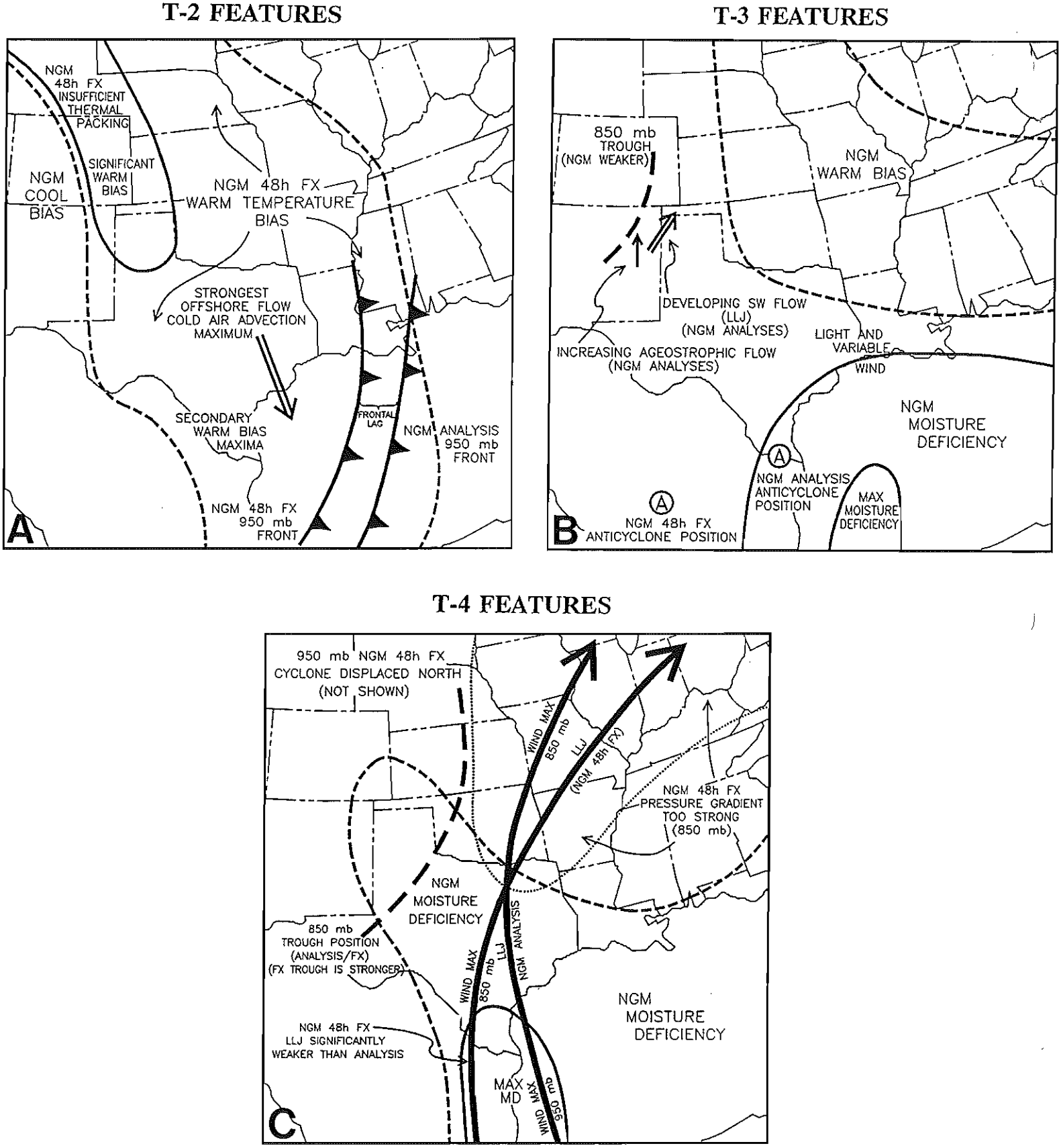

Fig. 9. Schematic diagrams of NGM strengths and weaknesses during the return flow cycle. Verification periods T-2, T-3, and T-4 are shown in Figs 9a, b, and c, respectively).